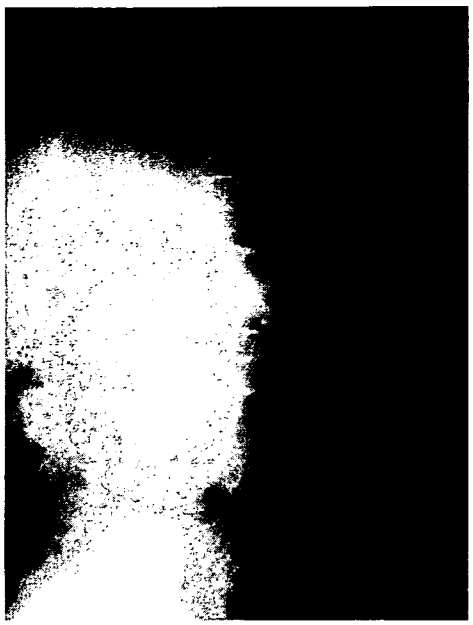

図1-a 初診時の単純X線腰椎側面像において第1腰椎の楔状化，局所後弯，遷延骨癒合とvacuum cleftを認めた．

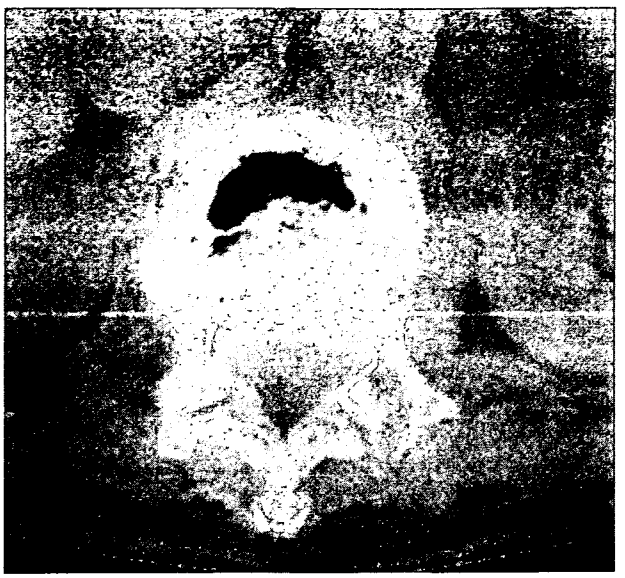

図1-b CT水平像では後壁骨折とそれに伴う骨片の脊柱管内転位，椎弓根基部での骨折，椎体前方でのvacuum cleftを認めた．

男性1例の合計7例(39.0%)であった．性別でみると，女性は15例中6例の40%，男性は3例中1例で33.3%の合併率であった．7例中，動作時痛の強かった3例中2例は軟性コルセットから硬性コルセットに変更し入院安静加療とした．この2例は約2カ月で動作時痛が軽快した．また，もう1例は第5腰椎に対して経椎弓根的にHAブロックを充填する椎体形成術を施行した．術後1カ月で疼痛軽快し歩行可能となったが，経時的に椎体圧潰を認めている．下肢の神経障害を呈していた4例は全例後壁骨折を合併しており，そのうちの2例には胸腔鏡視下前方除圧固定術(VATS)と後方固定術が施行され術後神経症状は改善した．しかし，椎体間ケージの頭尾側椎体へのmigrationによる局所後弯が認められている．また，1例は後方骨切り短縮固定術を施行し術後3カ月で歩行器移動が可能なまでに改善した．しかし，術後6カ月で頭側隣接椎体の楔状変形を認めた．残りの1例は硬性コルセットによる入院加療後2カ月で疼痛，筋力低下の改善が得られた．後壁骨折のなかった11例中，動作時痛が重症であった1例に経椎弓根的な骨セメント(PMMA)注入による椎体形成術を1例に施行し，疼痛の速やかな改善が得られた．椎弓根スクリューとフックによる後方固定術を施行した1例も術後3カ月で疼痛の軽快をみた．残りの9例は硬性コルセットによる自宅もしくは入院加療としたが，2～5カ月で体動時の疼痛改善を認めた．

Ⅲ．症　例

症例1：76歳，女性．自宅内で転倒後背部痛出現し近医にて2週間の安静入院加療を受けていた．その後退院するも歩行能力の低下や頻回の転倒を認め，パーキンソン病の増悪を疑われ当院神経内科に精査加療目的で入院した．受傷後3カ月の時点で動作時の背部痛と両下肢に徒手筋力テスト(MMT)で3程度

T1強調画像　　T2強調画像

図1-c,d　MRI矢状断像では第1腰椎腹側にT1，T2にて低輝度を示す椎体内ガスの存在，椎体中央頭側にはT1低～等輝度，T2高輝度を示す椎体内貯留液の存在，椎体頭背側部の骨片の脊柱管内への転位と脊髄円錐部の圧迫を認めた．また，第12胸椎の第1腰椎に対する後方亜脱臼を認めた．

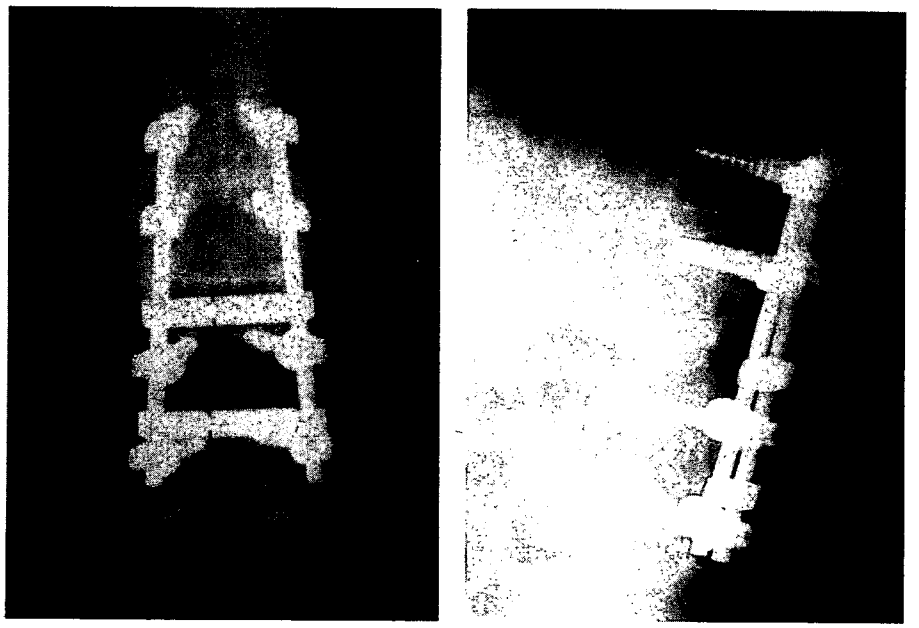

術後単純X線正面像　　術後単純X線側面像

図1-e,f　第1腰椎後方骨切り短縮固定術を施行．第11,12胸椎，第2,3腰椎の椎弓根内にハイドロキシアパタイト顆粒の充填後スクリューを刺入し固定性の強化を図った．

の筋力麻痺を認めていた．単純X線腰椎側面像において第1腰椎の楔状化，局所後弯，遷延骨癒合とvacuum cleftを認めた．CT水平像では後壁骨折とそれに伴う骨片の脊柱管内

CT矢状断像

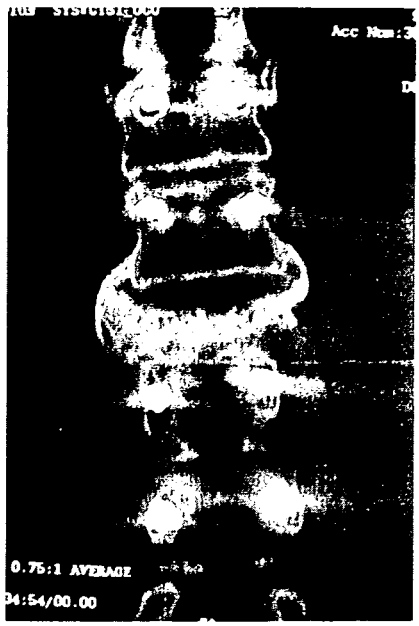

CT冠状断像

図1-g,h 術後7カ月のCT画像では矢状断では前縦靭帯に沿った仮骨と冠状断では椎体両側面での骨架橋による隣接椎体間の骨癒合が観察できた.

図1-i 術後7カ月の単純X線側面像では頭側隣接椎体(第10胸椎)の楔状変形を認めた.

転位，椎弓根基部での骨折を認めた．MRI矢状断像では第1腰椎腹側にT1，T2にて低輝度を示す椎体内ガスの存在，椎体中央頭側にはT1低～等輝度，T2高輝度を示す椎体内貯留液の存在，椎体頭背側部の骨片の脊柱管内への転位と脊髄円錐部の圧迫を認めた．また，第12胸椎の第1腰椎に対する後方亜脱臼を認めた．全身麻酔下に第1腰椎後方骨切り短縮固定術を施行．第11, 12胸椎，第2, 3腰椎の椎弓根内にハイドロキシアパタイト顆粒の充填後スクリューを刺入し固定性の強化を図った．術後3カ月で歩行器移動が可能となった．術後7カ月のCT画像では矢状断では前縦靭帯に沿った仮骨と冠状断では椎体両側面での骨架橋による隣接椎体間の骨癒合が観察できた．しかし，頭側隣接椎体(第10胸椎)の楔状変形を認めた(図1)．

症例2：87歳，女性．庭仕事をしていて徐々に背部痛と後弯変形に気づいていた．近医でリハビリするも改善なく症状発現後3カ月で当科を初診．MRIにて第1腰椎の椎体内vacuum cleftと脊柱管内への膨隆を認めた．しかし，後壁骨折は認めなかった．硬性コルセット固定で入院加療としたところ，約2カ月後で体動時痛が消失し軟性コルセットで外来通院とした．当科受診後5カ月のCTでは第2, 3腰椎にも新たな圧迫骨折を認めたが，自覚するほどの背部痛は訴えていなかった．また，第12胸椎から第2腰椎にかけて前縦靭帯に沿った仮骨形成を認めた．当科受診後8カ月の単純X線側面像ではこの仮骨の増大化を認めた(図2)．

Ⅳ. 考　察

福田ら[1]は疼痛発症日がほぼ明らかで体動困難なため入院治療した82例を対象とし，3週間の体幹ギプス固定後軟性もしくは硬性コルセット治療としたところ，治療開始時期が疼痛発症から14日以内とそれ以降では，4週後の疼痛および最終時局所後弯角，圧潰率，

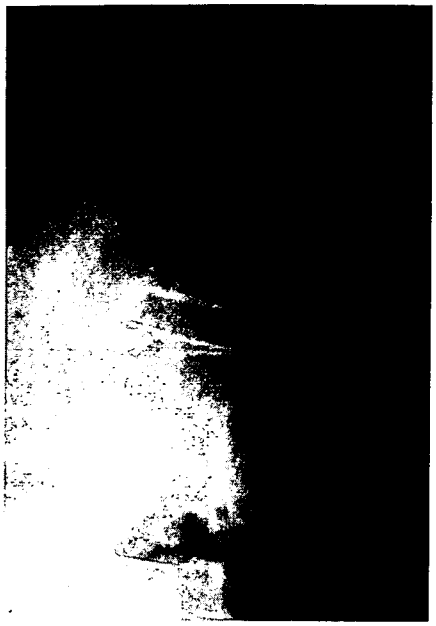

図2-a 初診時単純X線側面像では第1腰椎の楔状化と後弯，第4腰椎の前方すべりを認めた．

T1強調画像

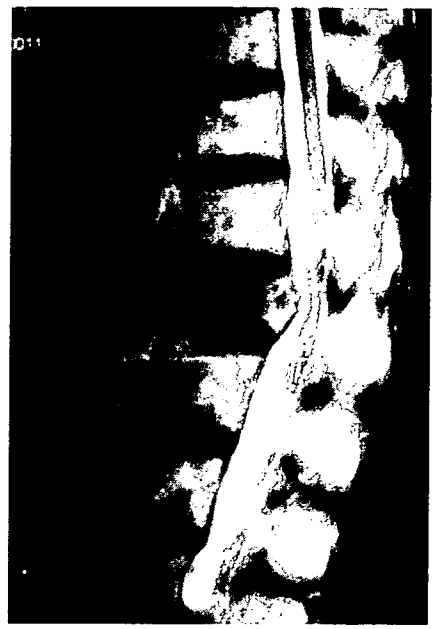

T2強調画像

図2-b,c MRI T1, T2強調画像では第1腰椎の椎体内vacuum cleftと脊柱管内への膨隆を認めた．しかし，後壁骨折は認めなかった．

図2-d 当科受診後5カ月のCTでは第2, 3腰椎にも新たな圧迫骨折を認めたが，自覚するほどの背部痛は訴えていなかった．また，第12胸椎から第2腰椎にかけて前縦靱帯に沿った仮骨形成を認めた．

図2-e 当科受診後8カ月の単純X線側面像ではこの仮骨の増大化を認めた．

偽関節発生率で後者の方が増悪傾向にあったと報告している．また，偽関節の危険因子の1つとしてあげられる後壁損傷の発生率は治療開始時期が疼痛発症から14日以内とそれ以降で有意差は認めなかったとしている．このときの後壁損傷とはMRIで椎体後壁の膨隆を認めたものとしている．つまり，後壁損傷は受傷時にすでに発生しており，後日に

徐々に発生するものではないといえる．後壁損傷の発生率に有意差がないのに偽関節発生率に増悪傾向の差があったということは，増悪因子に後壁損傷が関与していなかったか，もしくは同じ後壁損傷でも生体力学的な安定性に差が存在する可能性が考えられる．一方，加藤ら[2]は骨粗鬆症性椎体骨折による遅発性麻痺の成因として破裂骨折型と圧迫骨折型を提唱しているが，破裂骨折型のなかには受傷時は圧迫骨折であったものがその後の椎体圧潰により破裂骨折型となるものがあるとして，福田らと異なる結果を報告している．これはやはり圧迫骨折後にmidcolumnの支持性が徐々に低下していく可能性を示している．中野ら[3]は後壁損傷を伴う椎体骨折37症例を対象に初診後4カ月時点における疼痛で評価したところ，安静固定開始を直ちに行ったものでは良好であったが，初期固定が不適切なものでは不良であったとしている．また，後壁損傷のある椎体骨折は若年者より骨粗鬆症による高齢者に絶対数が多く，高齢者の骨折で特に軽微な外力で発生した場合は見逃すことが多いと報告している．つまり，後壁損傷は受傷後適切な治療が行われなければ，時間が経過するに従って骨安定性が低下していき，骨癒合率が低下し疼痛の残存となる可能性がある．吉川ら[4]は後壁損傷を伴った骨粗鬆症性脊椎圧迫骨折15例について経時的にMRI，CTにてその画像変化を検討したところ，受傷後1カ月間は物理的不安定性および生物学的骨吸収の亢進により骨量が減少する傾向にあったとし，この期間はとくに慎重な治療と経過観察が必要であると述べている．

今回提示した症例1では明らかに椎体後頭側に骨折線と骨片の転位を認めていたが，症例2では椎体後壁は脊柱管内へ頭尾側対称的な弧状に膨隆はしていたものの骨折線は認めていなかった．このため，症例2では安定性を維持でき，保存的加療でも良好な骨性架橋を得ることができたと考える．骨性架橋の評価にはCTが有用であるが，水平断のみでは椎体腹側，側壁の評価が困難であるため，矢状断と冠状断の画像が必要不可欠である．後壁骨折の発生機序であるが，骨粗鬆症性新鮮圧迫骨折を見逃され痛みを我慢しながら日常生活を送っていると椎体腹側の圧潰率や椎体後弯が進む．すると受傷椎体の頭側隣接椎体は後弯が増強するため前方にすべろうとする力が働く．このとき患者が後弯位から中間位へと起き上がろうとすると頭側隣接椎体による受傷椎体の後上縁に背尾側への剪断力が働き後壁頭側に骨折を生じさせるものと推測する(図1-c)．そうなると不安定性，遷延治癒，偽関節という状態に陥り頑固な疼痛や神経麻痺が発生しやすくなると考える．

遅発性神経麻痺に対する治療法について伊田ら[5]は，コルセットなどの保存的な治療法を選択した5例全例に麻痺の改善がみられたと報告している．その理由として，安静臥床していたために麻痺の程度が徒手筋力テストがMMTで3以下にならなかったためとしている．しかし，麻痺の改善がみられるようになった時期は保存療法開始後1～11カ月で平均6カ月であった．今回のシリーズでは手術治療した症例は1～3カ月で症状の改善を認めていることを考えると，症例1のような保存療法に抵抗する場合は，全身状態などが許されるのであれば手術療法も選択肢の1つになるのではないかと考える．骨粗鬆症性脊椎に対する手術療法であるが，強固な固定術を施行すると隣接椎体へ影響を及ぼしたり，固定材料の緩みやなどを考慮しなくてはならな

い．よって，術後も硬性コルセットなどの外固定は重要である．また，前方，後方いずれにしろ大きな展開での進入や長時間の手術は高齢患者に対して大きな侵襲となり合併症を伴う可能性が高くなる．経椎弓根的に骨セメントやペースト，HAを充填するいわゆる「経皮的椎体形成術」という術式は，低侵襲で即時的改善をもたらす治療法として最近本邦にても報告[6]が散見されるが，これは平成15年6月25日に「項番57：腫瘍性骨病変及び骨粗鬆症に伴う骨脆弱性病変に対する経皮的骨形成術(転移性脊椎骨腫瘍，骨粗鬆症による脊椎骨折又は難治性疼痛を伴う椎体圧迫骨折若しくは臼蓋骨折に係るものに限る)」として高度先進医療として認定されており，混合診療として実施することができるのは極めて限られた施設だけとなっている．とくに骨セメント(PMMA)は椎体に用いることがまだ承認されていない材料なため適応はいまだ慎重であるべきであると考える．

結　語

1）症状発症後3カ月経過後も症状の改善のない骨粗鬆症性椎体骨折18例を経験したので報告した．

2）18例中女性6例，男性1例の合計7例(39.0%）に後壁骨折を認めた．下肢の神経障害を合併した4例は全例に後壁骨折を認めた．

3）後壁の膨隆変形のみの後壁損傷は後壁骨折よりも整体力学的な安定性があると考えられ，保存療法でも良好な改善を得られる可能性がある．

文　献

1）福田文雄，大塚弘剛，益本真太郎，他：治療開始時期の違いによる骨粗鬆症性椎体骨折の予後—疼痛・椎体変形・偽関節の推移．別冊整形外科50：117–119, 2006
2）加藤浩三，芝啓一郎：骨粗鬆性椎体骨折による遅発性麻痺の成因と治療．整形・災害外科41：1555–1561, 1998
3）中野哲雄，安部靖之，清水泰宏，他：後壁骨折をともなう椎体骨折の保存療法—骨粗鬆症例を中心に．骨折23：45–48, 2001
4）吉川　啓，小坂泰啓，浦山茂樹，他：骨粗鬆症性脊椎圧迫骨折の経時的画像変化—とくに後壁損傷例について—．骨折26：59–64, 2004
5）侭田敏且，飯島卓夫：骨粗鬆症性椎体骨折による遅発性神経麻痺の保存的治療．整形外科56：1367–1371, 2005
6）南里康弘：内視鏡的経皮経椎弓根的椎体形成術—リン酸カルシウム骨ペースト椎体内注入療法．別冊整形外科50：126–134, 2006

*　　*　　*

Available online at www.sciencedirect.com
ScienceDirect
Biochemical and Biophysical Research Communications 353 (2007) 147–151
BBRC
www.elsevier.com/locate/ybbrc

FGF23 induces expression of two isoforms of NAB2, which are corepressors of Egr-1

Toru Fukuda [a], Kazuhiro Kanomata [a], Junya Nojima [a], Itaru Urakawa [b], Tetsuo Suzawa [c], Mana Imada [c], Akiko Kukita [d], Ryutaro Kamijo [c], Takeyoshi Yamashita [b], Takenobu Katagiri [a,*]

[a] *Division of Pathophysiology, Research Center for Genomic Medicine, Saitama Medical University, Yamane 1397-1, Hidaka-shi, Saitama 350-1241, Japan*
[b] *Pharmaceutical Research Laboratories, Pharmaceutical Division, Kirin Brewery Co., Ltd, Takasaki, Gunma 370-1295, Japan*
[c] *Department of Biochemistry, School of Dentistry, Showa University, Hatanodai 1-5-8, Shinagawa-ku, Tokyo 142-8555, Japan*
[d] *Department of Pathology and Biodefense, Faculty of Medicine, Saga University, Saga 849-8501, Japan*

Received 14 November 2006
Available online 11 December 2006

Abstract

Fibroblast growth factor 23 (FGF23) is a key humoral factor in phosphate homeostasis and skeletogenesis, though the nature of its intracellular signaling is still unclear. Recently, Egr-1, a zinc-finger transcription factor, was identified as an immediate early response gene of FGF23 in the kidney. We report here, that FGF23 induces not only Egr-1 but also two isoforms of NAB2, which are specific co-repressors of Egr-1. Both isoforms of NAB2 induced by FGF23 were localized in the nucleus and suppressed the transcriptional activity of Egr-1. A negative feedback loop established by Egr-1 and NAB2 may thus be involved in mediating the physiological effects of FGF23.

Keywords: FGF23; Egr-1; NAB2; Co-repressor; Transcription

Fibroblast growth factor 23 (FGF23) is a member of the FGF family and a key humoral factor in phosphate homeostasis and skeletogenesis [1–4]. Elevation of serum levels of FGF23 causes hypophosphatemia and skeletal abnormalities in patients who have mutations of the FGF23 gene or tumor cells over-expressing FGF23, such as those with autosomal-dominant hypophosphatemic rickets, tumor-induced osteomalacia, and X-linked hypophosphatemia [5–7]. FGF23 activity is regulated by proteases and its specific receptors. Mature FGF23 is degraded to two small fragments by furin family proteases [8]. Recently, Klotho and FGF type I receptors were identified as binding and signaling receptors, respectively [9,10]. Although FGF type I receptors are widely expressed in various tissues, systemically administered FGF23 acts only in the kidney [10]. Klotho, which is abundantly expressed in the kidney, appears to be a specific regulator of the activation of FGF23 signaling [10]. However, the intracellular signaling of FGF23 through these receptors remains to be clarified.

Early growth response-1 (Egr-1), also termed nerve growth factor-induced clone A (NGFI-A) or Krox-24, is an immediate early response transcription factor with zinc-finger motifs [11–13]. Egr-1 couples extracellular signals to the induction of cellular programs for differentiation, growth, and cell death [11,14]. Transcription of Egr-1 has been observed during osteoblast differentiation and tooth development, suggesting that Egr-1 plays important roles in bone and teeth [15,16].

Abbreviations: FGF, fibroblast growth factor; Egr-1, early growth response-1; NGFI-A, nerve growth factor-induced clone A; NAB, NGFI-A binding; NCD, NAB conserved domain.

* Corresponding author. Fax: +81 42 985 7214.
E-mail address: katagiri@saitama-med.ac.jp (T. Katagiri).

0006-291X/$ - see front matter © 2006 Elsevier Inc. All rights reserved.
doi:10.1016/j.bbrc.2006.12.011

The transcriptional activity of Egr-1 is negatively regulated by constitutive and inducible co-repressors, NGFI-A-binding protein (NAB) 1 and 2, respectively [13,17–21], which have highly conserved regions in their N-terminal and C-terminal portions termed NAB conserved domains (NCD) 1 and 2, respectively. It has been proposed that NCD1 is required for both interaction with Egr-1 and homo-oligomerization [11], and that NCD2 is essential for transcriptional repression [22,23]. The repressive function of NAB2 is mediated through two independent domains. The chromodomain helicase DNA-binding protein 4 interacting domain (CID) is recruited into the nucleosome remodeling and deacetylase complex through direct interaction. NCD2 is an independent repressive domain of NAB2 that exerts its repressive function through unidentified HDAC-independent mechanisms [24]. In contrast to full-length NAB2, an alternative form lacking exon 3 (NAB2ΔE3) lost repressive capacity due to disruption of NCD2 and a nuclear localization signal [12]. Egr-1 directly activates the promoter activity of NAB2 and thereby establishes a negative feedback loop to suppress extracellular signaling [25].

Recently, Egr-1 was identified as one of the immediate early target genes of FGF23 signaling in the kidney *in vivo* [10]. This finding suggested that an Egr-1-dependent pathway plays an important role in intracellular signaling through FGF23 receptors. In the present study, we found that FGF23 induced not only Egr-1 but also two isoforms of NAB2, a full-length form and one lacking exon 6 (NAB2ΔE6). In contrast to NAB2ΔE3, NAB2ΔE6 exhibited sustained capacity to suppress the transcriptional activity of Egr-1 as a full-length form of NAB2. Taken together, these findings suggest that the negative feedback loop established by Egr-1 and NAB2 may play roles in mediating the physiological effects of FGF23 in phosphate homeostasis and skeletogenesis.

Materials and methods

Administration of FGF-23 in vivo and in vitro. Balb/c mice at 6 weeks of age were i.p. injected with FGF23 at 20 μg/head. After 0.5 h, the kidney was removed under anesthesia and total RNA was extracted. HEK293T cells were treated with conditioned medium containing human FGF23 prepared by transient transfection of an expression vector carrying human FGF23 with R176Q and R179Q mutations in COS7 cells. Concentrations of FGF23 in conditioned medium were determined with a FGF23 ELISA kit (KAINOS, Tokyo, Japan).

Reverse transcription-polymerase chain reaction (RT-PCR). RT-PCR was performed using total RNA as described [26]. The primers used were as follows: human NAB2, 5′-tggccgtttcgactctaagc-3′ (forward) and 5′-caggacatctgtccagcagc-3′ (reverse), mouse NAB2, 5′-gacgatcatgacgcccag-3′ (forward) and 5′-cttcccccactttcactgcc-3′ (reverse), human Egr-1, 5′-gacagcagtcccatttactc-3′ (forward) and 5′-atcttggtatgcctcttgcg-3′ (reverse), mouse Egr-1, 5′-cttaataccacctactaccaatcccagc-3′ (forward) and 5′-gttgaggtgctgaaggagctgctga-3′ (reverse).

Co-immunoprecipitation and immunoblotting. For immunoprecipitation, cells were co-transfected with expression vectors for FLAG-mouse Egr-1 and Myc-mouse NAB2 proteins using Lipofectoamine 2000 transfection reagent (Invitrogen, Carlsbad, CA) according to the manufacturer's instructions. After 20 h, the cells were lysed in buffer [10 mM Tris–HCl (pH 7.5), 1% Triton X-100, 0.15 M NaCl, 1× protease inhibitor cocktail] and supernatants of the extracts were immunoprecipitated with anti-FLAG M2 agarose beads (Sigma–Aldrich, St. Louis, MO). After repeated washing with the lysis buffer, precipitates were subjected to immunoblotting using anti-Myc antibody (clone 9E10, Santa Cruz Biotechnology, Santa Cruz, CA).

Immunohistochemical staining. Immunohistochemical staining was performed as described. In brief, cells co-transfected with expression vectors for FLAG- and His-tagged proteins were fixed with 10% formalin 18 h later and doubly stained with anti-FLAG (clone M2, Sigma–Aldrich) and anti-Myc (MBL Medical & Biological Laboratories Co., Nagoya, Japan) antibodies.

Luciferase activity. Cells were co-transfected with expression vectors for Egr-1 and NAB2 with Id985-luc carrying a Egr-1 consensus sequence and pRL-SV40 (Promega, Madison, WI) using Lipofectamine 2000 (Invitrogen) as described previously [27]. After 20 h, luciferase activity was determined using a Dual Luciferase assay kit (Promega).

Results

FGF23 induces expression of NAB2 in vivo and in vitro

Recently, Egr-1 was identified as an immediate early response gene of FGF23 in the kidney [10]. We found that administration of FGF23 stimulated two transcripts of NAB2 of different sizes in the mouse kidney within 0.5 h (Fig. 1A). Stimulation of these NAB2 transcripts by FGF23 was also detected at 2 h in HEK293T cells with over-expression of exogenous Klotho (Fig. 1B). In these cells, Egr-1 mRNA was also induced within 0.5 h by FGF23 (Fig. 1B). Determination of DNA sequences of the long and short transcripts of NAB2 indicated that they were the full-length (NAB2full) and an alternatively spliced form of NAB2 lacking exon 6 (NAB2ΔE6), respectively (Fig. 1C). The transcripts of both NAB2full and NAB2ΔE6 were ubiquitously expressed in various tissues in mice (Fig. 1D). We detected no isoform of NAB2 lacking exon 3 (NABΔE3) in any types of cells examined (data not shown).

Cellular localization and functions of two types of NAB2 isoforms

Immunoprecipitation followed by Western blot analysis indicated that both NAB2full and NAB2ΔE6 interacted with Egr-1 and formed homo- and hetero-oligomers with each other (Fig. 2A). However, neither NAB2full nor NAB2ΔE6 exhibited capacity to interact with osterix, another type of C2H2 zinc-finger protein (Fig. 2A). Transient over-expression of Myc-tagged NAB2full or NAB2ΔE6 with FLAG-tagged Egr-1 indicated that all of these proteins were localized in the nucleus, suggesting that they had formed complexes in the nuclei (Fig. 2B). Both NAB2full and NAB2ΔE6 suppressed the transcriptional activity of Egr-1 (Fig. 2C).

A previous study revealed that a point mutation of E51K in NCD1 in mouse NAB1 interfered with its ability to bind to Egr-1 [17]. We therefore introduced the corresponding mutation, E82K, into mouse NAB2full and

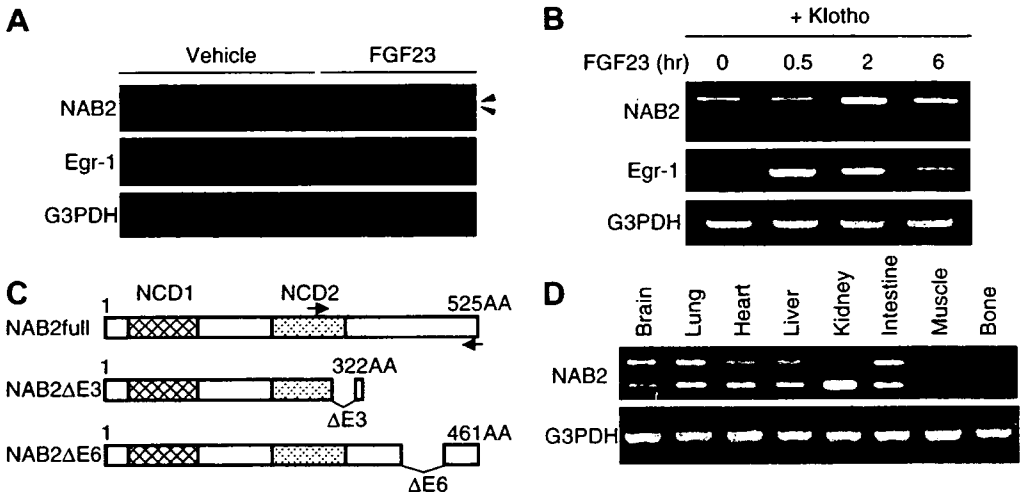

Fig. 1. FGF-23 induced NAB2 expression. (A) FGF23 induced expression of Egr-1 and NAB2 in mouse kidney. Mice were injected i.p. with FGF23 at 20 μg/head, and then total RNA was prepared from the kidney after 0.5 h. RT-PCR analysis was performed for Egr-1, NAB2, and G3PDH. (B) FGF23 induced transcription of both Egr-1 and NAB2 *in vitro*. HEK293T cells with Klotho over-expression were treated with conditioned medium containing FGF23 for the indicated period. RT-PCR analysis was performed for Egr-1, NAB2, and G3PDH. (C) Schematic structures of three isoforms of NAB2, NAB2full, NAB2ΔE3, and NAB2ΔE6. Two independent, highly conserved domains in NAB proteins are indicated as NCD1 and NCD2. Primers used in RT-PCR analysis are indicated by arrows. (D) RT-PCR analysis of NAB2 mRNAs in various tissues of mice.

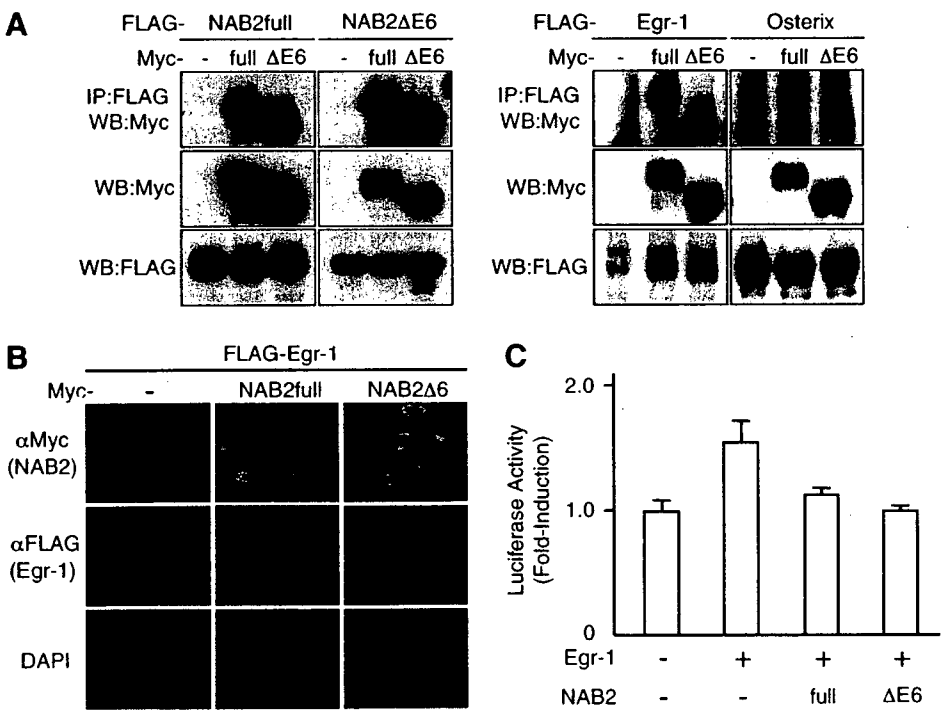

Fig. 2. Comparison of properties of NAB2full and NAB2ΔE6. (A) Interactions of NABfull and NAB2ΔE6 and Egr-1. FLAG-tagged NAB2full, NAB2ΔE6, Egr-1 or Osterix and Myc-tagged NAB2full or NAB2ΔE6 were co-transfected in COS7 cells, and then immunoprecipitated with anti-FLAG M2 agarose beads. The precipitates were subjected to Western blot analysis using anti-Myc antibody. (B) Cellular location of NABfull or NAB2ΔE6 and Egr-1. Myc-tagged NAB2full or NAB2ΔE6 was co-transfected with FLAG-tagged Egr-1 in HEK293T cells. The cells were immunohistochemically stained with anti-FLAG and anti-Myc antibodies. (C) NAB2full and NAB2ΔE6 suppressed the transcriptional activity of Egr-1. A luciferase reporter carrying an Egr-1 consensus sequence was co-transfected with NAB2full or NAB2ΔE6 in the presence of Egr-1. Luciferase activities were determined using a kit.

NAB2ΔE6 and examined their properties. The E82K mutation abolished the abilities of both NAB2full and NAB2ΔE6 to bind to Egr-1, though they were still able to form homo- and hetero-oligomers with each other (Fig. 3A). Immunohistochemical analysis indicated that these E82K mutants of NAB2, especially NAB2ΔE6(E82K), formed snake-like structures in the nuclei, although Egr-1 was distributed homogeneously in

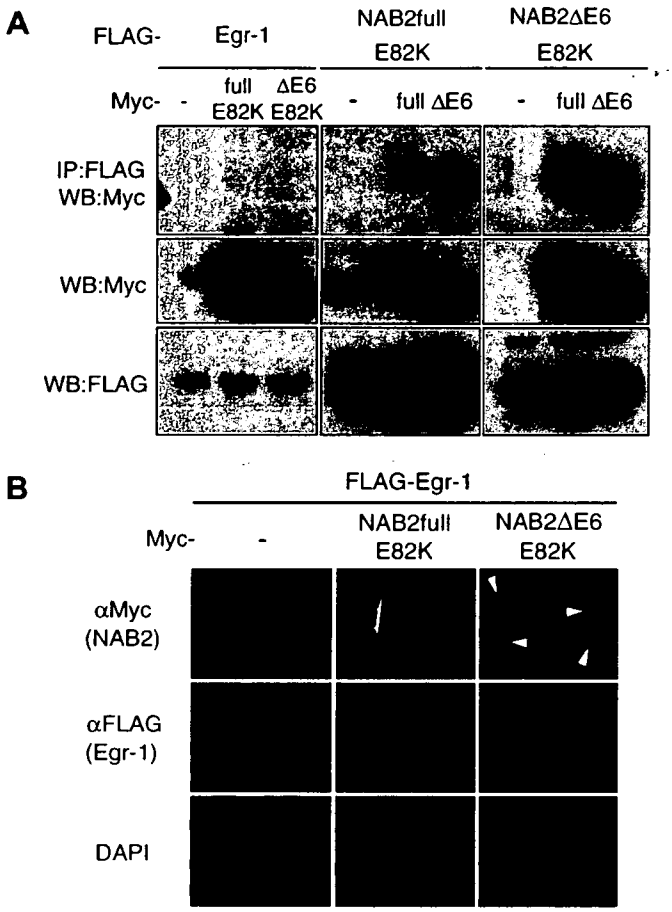

Fig. 3. Characterization of properties of NAB2full and NAB2ΔE6 with E82K mutation. (A) Interactions of NABfull(E82K) and NAB2-ΔE6(E82K) with Egr-1. FLAG-tagged Egr-1 and Myc-tagged NAB2full(E82K) or NAB2ΔE6(E82K) were co-transfected in COS7 cells, and then immunoprecipitated with anti-FLAG M2 agarose beads. The precipitates were subjected to Western blot analysis using anti-Myc antibody. (B) Cellular location of NABfull(E82K) or NAB2ΔE6(E82K) and Egr-1. Myc-tagged NAB2full(E82K) or NAB2ΔE6(E82K) was co-transfected with FLAG-tagged Egr-1 in HEK293T cells. The cells were immunohistochemically stained with anti-FLAG and anti-Myc antibodies. Typical snake-like structures are indicated by the arrowheads.

the nucleus (Fig. 3B). Thus, the location of the E82K mutant proteins of NAB2 differed completely from that of Egr-1.

Discussion

FGF23 is an important factor in phosphate homeostasis and skeletogenesis in vertebrates [2–4]. Although the molecular mechanisms in FGF23 signaling have not been elucidated, Klotho and FGF type I receptors were recently identified as specific receptors for FGF23 [9,10]. In addition, recent work revealed that FGF23 induced Egr-1 expression as an immediate early response gene in the kidney *in vivo* [10]. In the present study, we found that FGF23 induced expression of not only Egr-1 but also NAB2 *in vivo* and *in vitro* in the presence of Klotho. Mice doubly deficient in NAB1 and NAB2 exhibited abnormalities in various tissues, including the skeleton [28]. It has been reported that Egr-1 directly activates the promoter activity of NAB2 [25]. Taken together, these findings suggested that FGF23 induces Egr-1 and then NAB2 in a negative feedback loop to suppress its own signaling. Egr-1- and NAB2-dependent intracellular signaling may play roles in mediating the physiological effects of FGF23, such as phosphate homeostasis and skeletogenesis. This possibility can be tested by administration of FGF23 to Egr-1 or NAB2-deficient mice in the future.

We found that FGF23 induced two isoforms of NAB2 transcripts, a full-length form and an alternative spliced one lacking exon 6, NAB2ΔE6. Another form of NAB2 lacking exon 3, NAB2ΔE3, had been detected in the cytoplasm and had lost the ability to inhibit the transcriptional activity of Egr-1 due to disruption of NCD2 and nuclear localization signal [12]. The present findings suggest that both NAB2full and NAB2ΔE6 are major forms of NAB2 in various tissues and cell lines. In contrast to NAB2ΔE3, however, NAB2ΔE6 had both complete NCD2 and nuclear localization domain and had retained the ability to bind to Egr-1 and suppress its transcriptional activity. These findings clearly indicated that NAB2ΔE6 is a functional isoform like full-length NAB2 and quite different from NAB2ΔE3. This was further confirmed by examination of NAB2ΔE6(E82K), which showed that it did not bind Egr-1. The cellular location of NAB2ΔE6(E82K) differed from Egr-1 in the nucleus, though NAB2ΔE6 was co-localized with Egr-1, suggesting that the interaction of NAB2-ΔE6(E82K) and Egr-1 had been disrupted by the point mutation *in vivo*.

In conclusion, we found a novel regulatory system for FGF23 signaling mediated though Egr-1 and NAB2. Further study of FGF23 signaling will provide new insights into the physiological roles of FGF23 in phosphate homeostasis and skeletogenesis.

Acknowledgments

We thank Dr. Yo-ichi Nabeshima for kindly providing a Klotho expression plasmid. This work was supported in part by the Ministry of Education, Culture, Sports, Science, and Technology of Japan, in particular by a Ministry Grant to the Saitama Medical University Research Center for Genomic Medicine.

References

[1] T. Yamashita, Structural and biochemical properties of fibroblast growth factor 23, Ther. Apher. Dial. 9 (2005) 313–318.
[2] M. Baum, S. Schiavi, V. Dwarakanath, R. Quigley, Effect of fibroblast growth factor-23 on phosphate transport in proximal tubules, Kidney Int. 68 (2005) 1148–1153.
[3] T. Shimada, M. Kakitani, Y. Yamazaki, H. Hasegawa, Y. Takeuchi, T. Fujita, S. Fukumoto, K. Tomizuka, T. Yamashita, Targeted ablation of Fgf23 demonstrates an essential physiological role of FGF23 in phosphate and vitamin D metabolism, J. Clin. Invest. 113 (2004) 561–568.

[4] M.S. Razzaque, D. Sitara, T. Taguchi, R. St-Arnaud, B. Lanske, Premature aging-like phenotype in fibroblast growth factor 23 null mice is a vitamin D-mediated process, FASEB J. 20 (2006) 720–722.
[5] K.E. White, G. Carn, B. Lorenz-Depiereux, A. Benet-Pages, T.M. Strom, M.J. Econs, Autosomal-dominant hypophosphatemic rickets (ADHR) mutations stabilize FGF-23, Kidney. Int. 60 (2001) 2079–2086.
[6] The ADHR Consortium, Autosomal dominant hypophosphataemic rickets is associated with mutations in FGF23, Nat. Genet 26 (2000) 345–348.
[7] A. Benet-Pages, P. Orlik, T.M. Strom, B. Lorenz-Depiereux, An FGF23 missense mutation causes familial tumoral calcinosis with hyperphosphatemia, Hum. Mol. Genet. 14 (2005) 385–390.
[8] S. Fukumoto, Post-translational modification of Fibroblast Growth Factor 23, Ther. Apher. Dial. 9 (2005) 319–322.
[9] H. Kurosu, Y. Ogawa, M. Miyoshi, M. Yamamoto, A. Nandi, K.P. Rosenblatt, M.G. Baum, S. Schiavi, M.C. Hu, O.W. Moe, M. Kuro-o, Regulation of fibroblast growth factor-23 signaling by klotho, J. Biol. Chem. 281 (2006) 6120–6123.
[10] I. Urakawa, Y. Yamazaki, T. Shimada, K. Iijima, H. Hasegawa, K. Okawa, T. Fujita, S. Fukumoto, T. Yamashita, Klotho converts canonical FGF receptor into a specific receptor for FGF23, Nature 444 (2006) 770–774.
[11] A. Gashler, V.P. Sukhatme, Early growth response protein 1 (Egr-1): prototype of a zinc-finger family of transcription factors, Prog. Nucleic Acid Res. Mol. Biol. 50 (1995) 191–224.
[12] J. Svaren, B.R. Sevetson, E.D. Apel, D.B. Zimonjic, N.C. Popescu, J. Milbrandt, NAB2, a corepressor of NGFI-A (Egr-1) and Krox20, is induced by proliferative and differentiative stimuli, Mol. Cell. Biol. 16 (1996) 3545–3553.
[13] B.R. Sevetson, J. Svaren, J. Milbrandt, A novel activation function for NAB proteins in EGR-dependent transcription of the luteinizing hormone beta gene, J. Biol. Chem. 275 (2000) 9749–9757.
[14] S.L. Lee, Y. Sadovsky, A.H. Swirnoff, J.A. Polish, P. Goda, G. Gavrilina, J. Milbrandt, Luteinizing hormone deficiency and female infertility in mice lacking the transcription factor NGFI-A (Egr-1), Science 273 (1996) 1219–1221.
[15] M. Ohba, M. Shibanuma, T. Kuroki, K. Nose, Production of hydrogen peroxide by transforming growth factor-beta 1 and its involvement in induction of egr-1 in mouse osteoblastic cells, J. Cell. Biol. 126 (1994) 1079–1088.
[16] I. Thesleff, A. Vaahtokari, P. Kettunen, T. Aberg, Epithelial–mesenchymal signaling during tooth development, Connect. Tissue Res. 32 (1995) 9–15.
[17] J. Svaren, B.R. Sevetson, T. Golda, J.J. Stanton, A.H. Swirnoff, J. Milbrandt, Novel mutants of NAB corepressors enhance activation by Egr transactivators, EMBO J. 17 (1998) 6010–6019.
[18] P. Houston, C.J. Campbell, J. Svaren, J. Milbrandt, M. Braddock, The transcriptional corepressor NAB2 blocks Egr-1-mediated growth factor activation and angiogenesis, Biochem. Biophys. Res. Commun. 283 (2001) 480–486.
[19] M. Lucerna, D. Mechtcheriakova, A. Kadl, G. Schabbauer, R. Schafer, F. Gruber, Y. Koshelnick, H.D. Muller, K. Issbrucker, M. Clauss, B.R. Binder, E. Hofer, NAB2, a corepressor of EGR-1, inhibits vascular endothelial growth factor-mediated gene induction and angiogenic responses of endothelial cells, J. Biol. Chem. 278 (2003) 11433–11440.
[20] Z. Qu, L.A. Wolfraim, J. Svaren, M.U. Ehrengruber, N. Davidson, J. Milbrandt, The transcriptional corepressor NAB2 inhibits NGF-induced differentiation of PC12 cells, J. Cell. Biol. 142 (1998) 1075–1082.
[21] F. Mechta-Grigoriou, S. Garel, P. Charnay, Nab proteins mediate a negative feedback loop controlling Krox-20 activity in the developing hindbrain, Development 127 (2000) 119–128.
[22] A.H. Swirnoff, E.D. Apel, J. Svaren, B.R. Sevetson, D.B. Zimonjic, N.C. Popescu, J. Milbrandt, Nab1, a corepressor of NGFI-A (Egr-1), contains an active transcriptional repression domain, Mol. Cell. Biol. 18 (1998) 512–524.
[23] M.W. Russo, B.R. Sevetson, J. Milbrandt, Identification of NAB1, a repressor of NGFI-A- and Krox20-mediated transcription, Proc. Natl. Acad. Sci. USA 92 (1995) 6873–6877.
[24] R. Srinivasan, G.M. Mager, R.M. Ward, J. Mayer, J. Svaren, NAB2 represses transcription by interacting with the CHD4 subunit of the nucleosome remodeling and deacetylase (NuRD) complex, J. Biol. Chem. 281 (2006) 15129–15137.
[25] J. Kumbrink, M. Gerlinger, J.P. Johnson, Egr-1 induces the expression of its corepressor nab2 by activation of the nab2 promoter thereby establishing a negative feedback loop, J. Biol. Chem. 280 (2005) 42785–42793.
[26] B. Zhao, T. Katagiri, H. Toyoda, T. Takada, T. Yanai, T. Fukuda, U.I. Chung, T. Koike, K. Takaoka, R. Kamijo, Heparin potentiates the in vivo ectopic bone formation induced by bone morphogenetic protein-2, J. Biol. Chem. 281 (2006) 23246–23253.
[27] T. Katagiri, M. Imada, T. Yanai, T. Suda, N. Takahashi, R. Kamijo, Identification of a BMP-responsive element in Id1, the gene for inhibition of myogenesis, Genes Cells 7 (2002) 949–960.
[28] N. Le, R. Nagarajan, J.Y. Wang, J. Svaren, C. LaPash, T. Araki, R.E. Schmidt, J. Milbrandt, Nab proteins are essential for peripheral nervous system myelination, Nat. Neurosci. 8 (2005) 932–940.

Available online at www.sciencedirect.com
ScienceDirect
ELSEVIER
Biochemical and Biophysical Research Communications 361 (2007) 62–67
BBRC
www.elsevier.com/locate/ybbrc

Platelet-rich plasma stimulates osteoblastic differentiation in the presence of BMPs

Akihiro Tomoyasu [a], Kanji Higashio [a,b], Kazuhiro Kanomata [a], Masaaki Goto [a,c], Kunihiko Kodaira [a,d], Hiroko Serizawa [a], Tatsuo Suda [a], Atsushi Nakamura [a], Junya Nojima [a], Toru Fukuda [a], Takenobu Katagiri [a,*]

[a] *Division of Pathophysiology, Research Center for Genomic Medicine, Saitama Medical University, 1397-1 Yamane, Hidaka-shi, Saitama 350-1241, Japan*
[b] *Metabolome Pharmaceuticals, Inc., 2-20-3 Nakamachi, Meguro-ku, Tokyo 153-0065, Japan*
[c] *Chugai Pharmaceutical Co., Ltd., Fuji Gotemba Research Laboratories, Genome Antibody Product Research Division, 1-135 Komakado, Gotemba, Shizuoka 412-8513, Japan*
[d] *Chugai Pharmaceutical Co., Ltd., Drug Engineering Division, 5-1, Ukima 5, Kita-ku, Tokyo 115-8543, Japan*

Received 25 June 2007
Available online 5 July 2007

Abstract

Platelet-rich plasma (PRP) is clinically used as an autologous blood product to stimulate bone formation in vivo. In the present study, we examined the effects of PRP on proliferation and osteoblast differentiation in vitro in the presence of bone morphogenetic proteins (BMPs). PRP and its soluble fraction stimulated osteoblastic differentiation of myoblasts and osteoblastic cells in the presence of BMP-2, BMP-4, BMP-6 or BMP-7. The soluble PRP fraction stimulated osteoblastic differentiation in 3D cultures using scaffolds made of collagen or hydroxyapatite. Moreover, heparin-binding fractions obtained from serum also stimulated osteoblastic differentiation in the presence of BMP-4. These results suggested that platelets contain not only growth factors for proliferation but also novel potentiator(s) for BMP-dependent osteoblastic differentiation.

Keywords: Bone morphogenetic proteins; Platelet-rich plasma; Osteoblasts; Scaffolds

Bone morphogenetic proteins (BMPs) have a unique and specific activity that is capable of inducing bone formation in vivo [1]. BMPs are responsible for not only artificial ectopic bone formation but also physiological skeletal development [2]. The bone-inducing activity of BMPs should be useful for the development of therapeutic drugs for in vivo bone regeneration [3,4]. However, it has been reported that, compared with rodents, more than 100-fold amounts of BMPs are required to induce bone formation in higher animals such as monkeys and humans [5]. We previously found that sulfated polysaccharides such as heparin and heparan sulfate enhanced BMP-induced osteoblast differentiation in vitro [6,7]. Moreover, heparin enhanced the ectopic bone formation in vivo induced by BMP-2 by protecting BMPs from degradation and inhibition by antagonists [6,7]. This finding suggests that BMP potentiators may be clinically useful for administration of BMPs to stimulate local bone formation in vivo.

Platelets are anuclear cells derived from megakaryocytes, and play important roles as rich sources of growth factors, including platelet-derived growth factor (PDGF), vascular endothelial growth factor, and transforming growth factor-β (TGF-β) [8,9]. These factors stored in α-granules of platelets are released through the activation of platelets by various stimuli [8,9]. Platelet-rich plasma (PRP) is clinically used as an autologous blood product to stimulate tissue regeneration in periodontal defects, extraction sockets, during implant placement, and in

* Corresponding author. Fax: +81 42 985 7214.
E-mail address: katagiri@saitama-med.ac.jp (T. Katagiri).

0006-291X/$ - see front matter © 2007 Elsevier Inc. All rights reserved.
doi:10.1016/j.bbrc.2007.06.142

guided bone regeneration around implants [8,9]. The capacity of PRP to stimulate bone regeneration is believed to be due to the stimulatory activities of the growth factors released from activated platelets on proliferation of progenitor cells and vascularization at local sites [8,9].

In the present study, we examined the effects of PRP on proliferation and osteoblastic differentiation in vitro in the presence of small amounts of BMPs, and found that PRP stimulated the osteoblastic differentiation. Moreover, a soluble fraction prepared from activated PRP also exhibited stimulatory effects on the BMP activity in 3D cultures on scaffolds. These findings suggest that simultaneous administration of BMPs and PRP with scaffolds is a simple and useful method of stimulating bone formation in vivo. They also suggest that platelets contain novel potentiator(s) of BMPs that stimulate osteoblastic differentiation of progenitor cells.

Materials and methods

Materials. Bovine plasma was purchased from Funakoshi, Tokyo, Japan. Dulbecco's modified Eagle's medium (DMEM) α-minimal essential medium (α-MEM) were obtained from Sigma–Aldrich (St. Louis, MO). Fetal bovine serum (FBS) and calf serum (CS) were obtained from Moregate Biotech (Bulimba, Qld, Australia). Bovine thrombin was obtained from Wako Pure Chemical Industries (Osaka, Japan). Recombinant BMP-2 produced in *Escherichia coli* was obtained from Acris Antibodies GmbH (Nordhein-Westfalen, Germany). Recombinant human BMP-4, BMP-6, and BMP-7 were purchased from R&D Systems (Minneapolis, MN). SuperScript III and Platinum Pfx DNA polymerase were from Invitrogen (Carlsbad, CA). Collagen sponge and porous hydroxyapatite (Celllyard, HA) were obtained from Wako Pure Chemical Industries and Pentax (Tokyo, Japan), respectively. A Cell Count Reagent SF kit was from Nacalai Tesque, Tokyo, Japan. Heparin sepharose CL-6B column was obtained from GE Healthcare (Fairfield, CT).

Cell cultures. A mouse cell line, C2C12, was maintained in DMEM containing 15% FBS [10], and ST-2, MC3T3-E1 and 3T3-L1 cells were maintained in α-MEM containing 10% FBS. C2C12 cells were inoculated at 1.0×10^4 cells/well in type I collagen-coated 96-well plates (IWAKI, Tokyo, Japan) and cultured overnight before treatment with stimuli. ST-2, MC3T3-E1, and 3T3-L1 cells were inoculated at 500 cells/well in type I collagen-coated plates and cultured for 2 days. BMPs at various concentrations were added to the cultures in fresh medium containing 1% FBS with or without PRP or a soluble fraction prepared from PRP or platelet-poor plasma (PPP). Osteoblastic differentiation was determined by measuring alkaline phosphatase (ALP) activity and mRNA levels as described below.

Preparations of PRP and PPP, and soluble fractions of PRP and PPP. Human or bovine plasma was centrifuged at 2100*g* for 20 min to precipitate platelets. PRP was prepared by re-suspending the precipitates in 1/100 volume of PPP, which was the supernatant fraction derived from centrifugation of plasma. The PRP and PPP were diluted 1/10 in DMEM containing 1% FBS and then activated with 0.01 U/μl of bovine thrombin in the presence of 0.025% $CaCl_2$. The activated PRP and PPP were centrifuged at 3400*g* for 10 min to remove fibrin clots, and the supernatants were prepared as soluble fractions of PRP and PPP, respectively.

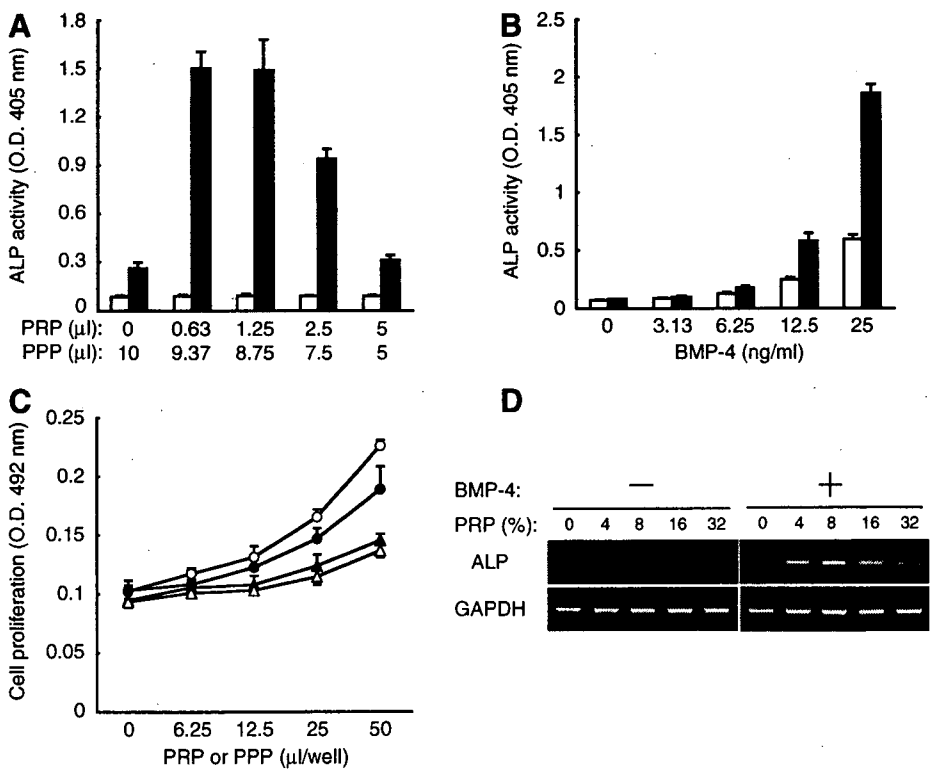

Fig. 1. Human and bovine PRP stimulate proliferation and osteoblastic differentiation of C2C12 myoblasts in the presence of BMP-4. (A) Human PRP diluted with PPP was added to cultures of C2C12 cells in the presence (solid bars) and absence (open bars) of 20 ng/ml of BMP-4. Total amount of the mixture was fixed at 10 μl in 150 μl of total culture volume. On day 6, ALP activity was determined as a marker of osteoblastic differentiation. (B) Soluble fraction prepared from bovine PRP (solid bars) or PPP (open bars) was added to C2C12 cultures with increasing concentrations of BMP-4. ALP activity was determined on day 4. (C) Effects of soluble PRP (circles) and PPP (triangles) fractions on proliferation of C2C12 cells in the presence (solid symbols) or absence (open symbols) of 25 ng/ml of BMP-4. Cell proliferation capacity was determined on day 4. (D) RT-PCR analysis of levels of expression of ALP mRNAs. C2C12 cells were treated for 4 days with increasing amounts of soluble PRP fraction in the presence or absence of 25 ng/ml of BMP-4.

Measurements of ALP activity and cell proliferation. ALP activity was measured as described previously [11]. In brief, the cells were rinsed with PBS and enzyme activity was determined by directly adding ALP buffer containing a substrate (0.6 M diethanolamine, 0.6 mM $MgCl_2$, 0.1% Triton X-100, and 30 mM *p*-nitrophenylphosphate) to each well. After incubation for 15 min at room temperature, the reaction was terminated by adding 3 M NaOH, and absorbance at 405 nm was measured using a microplate reader (ASYS Hitech Gmbh, Eugendorf, Austria). Cell proliferation was measured by absorbance at 492 nm using a Cell Count Reagent SF kit according to the manufacture's instructions.

Reverse transcription-polymerase chain reaction (RT-PCR). Levels of expression of ALP mRNA were analyzed by a RT-PCR technique as described [12]. In brief, cDNA was reverse transcribed from 5 μg of total RNA, and then each sequence was amplified by PCR (94 °C, 45 s; 60 °C, 1 min; 68 °C, 1 min; 30 cycles). Primers for ALP and glyceraldehyde-3-dehydrogenase were used [12].

Heparin sepharose CL-6B column chromatography. One liter of CS was pre-fractionated using a heparin sepharose CL-6B column equilibrated with 50 mM Tris–HCl, pH 7.5, containing 0.1% Chaps by a linear gradient of NaCl. This procedure was repeated five times. Fractions eluted with 1.0–1.5 M NaCl were pooled and applied to a new heparin sepharose CL-6B column. The bound proteins were eluted with a linear gradient of NaCl from 0 to 2.0 M. Each fraction was examined for ALP-inducing activity in C2C12 cells in the presence or absence of 20 ng/ml of BMP-4.

Results

PRP and soluble fraction of PRP stimulate BMP-4-induced osteoblastic differentiation and proliferation of C2C12 myoblasts

BMP-4 at 20 ng/ml slightly induced ALP activity in C2C12 cells (Fig. 1A). Addition of human PRP to the cultures stimulated ALP activity at lower concentrations, although the degree of stimulation gradually decreased at higher concentrations (Fig. 1A). In contrast, human PPP failed to stimulate ALP activity at all concentrations examined (Fig. 1A). We further examined the stimulatory activity in the soluble fractions prepared from bovine activated PRP and PPP. The ALP activity induced by BMP-4 at 12.5

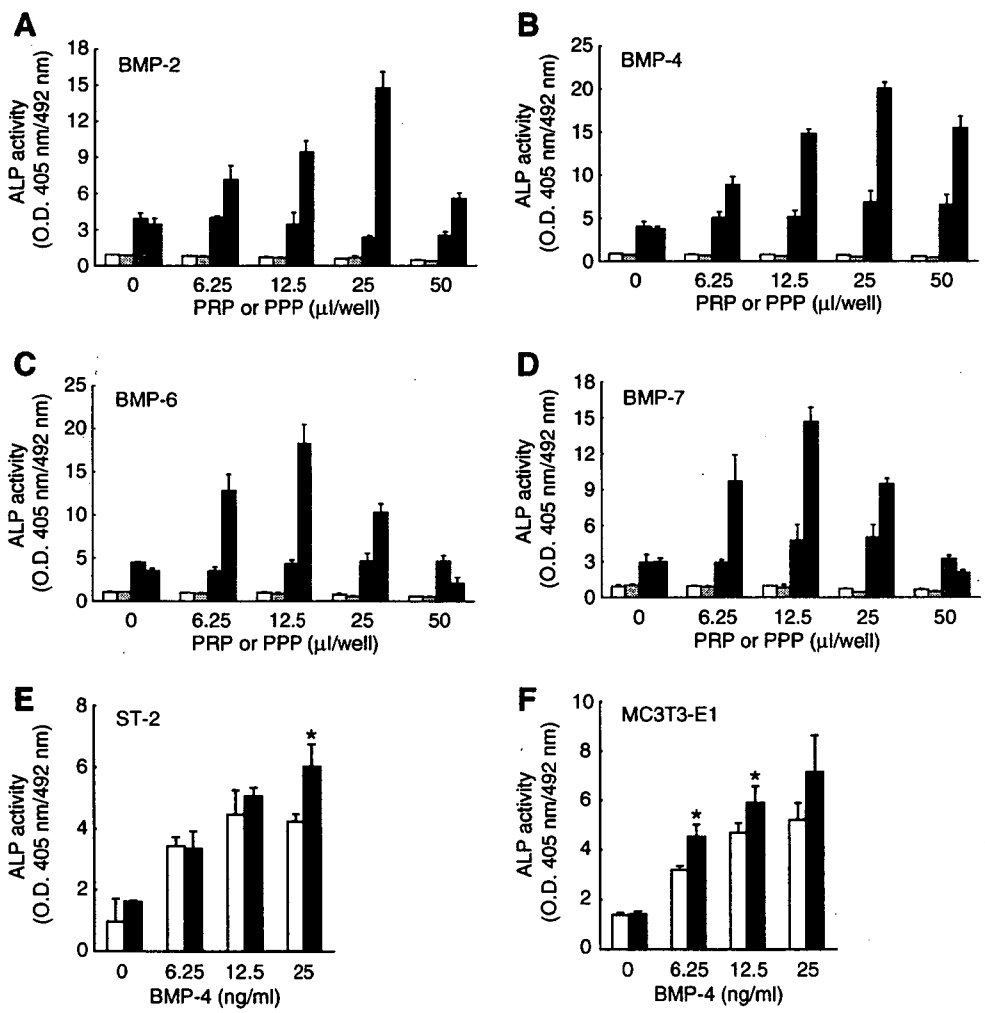

Fig. 2. Soluble PRP fraction stimulates osteoblastic differentiation of C2C12, ST-2, and MC3T3-E1 cells induced by various BMPs. Soluble fraction prepared from bovine PPP (open and gray bars) or PRP (light gray and solid bars) was added to cultures of C2C12 cells in the absence (open and light gray bars) or presence (gray and solid bars) of 300 ng/ml of BMP-2 (A), 25 ng/ml of BMP-4 (B), 150 ng/ml of BMP-6 (C), or 200 ng/ml of BMP-7 (D). ST-2 bone marrow stromal cells (E) and MC3T3-E1 osteoblasts (F) were cultured with graded concentrations of BMP-4 in the presence of soluble fraction prepared from bovine PPP (open bars) or PRP (solid bars). ALP activity was determined on day 4. $^*P < 0.05$ vs. PPP.

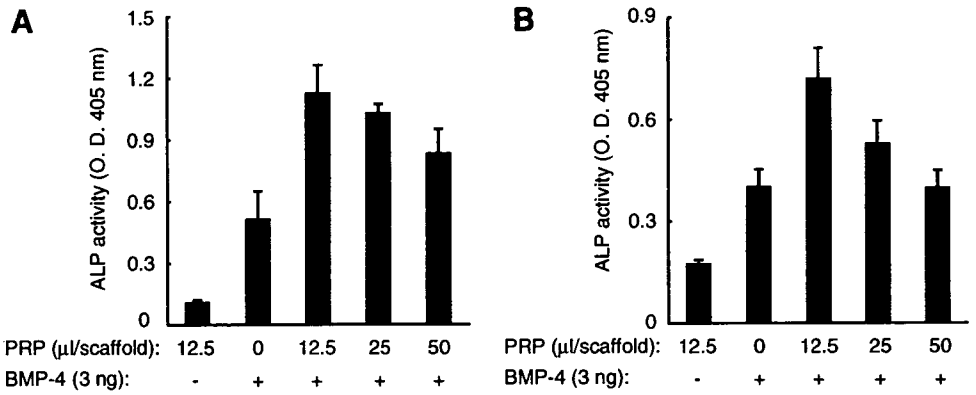

Fig. 3. Soluble PRP fraction and BMP-4 are retained in scaffolds and stimulate osteoblastic differentiation in vitro. Scaffolds made of collagen (A) and hydroxyapatite (B) were pre-incubated for 1 h with graded concentrations of soluble PRP fraction in the presence or absence of 3 ng of BMP-4 at room temperature, and then rinsed with PBS. C2C12 cells were inoculated on these scaffolds without additional PRP or BMP-4. ALP activity was determined on day 7.

and 25 ng/ml was much higher in the presence of the soluble fraction of PRP than that of PPP (Fig. 1B). Both soluble fractions of PRP and PPP stimulated proliferation at higher concentrations regardless of the presence of BMP-4, and higher stimulatory capacity was observed with the PRP fraction (Fig. 1C). The soluble PRP fraction increased levels of expression of ALP mRNA at lower concentrations in the presence of BMP-4 (Fig. 1D).

Ligand- and cell type-specificities of stimulatory activity of PRP

We examined the stimulatory effect of the soluble PRP fraction on osteoblastic differentiation in the presence of other BMPs. The soluble fraction of PRP, but not that of PPP, stimulated ALP activity in C2C12 cells in the presence of BMP-2, BMP-4, BMP-6, and BMP-7 (Fig. 2A–D). Higher concentrations of the soluble PRP fraction suppressed the ALP activity induced by each BMP examined, suggesting some inhibitors were also present in it. We next examined the stimulation of the BMP activity by the soluble fraction of PRP in two types of osteoblastic cells, ST-2 bone marrow stromal cells and MC3T3-E1 osteoblasts. In both types of cells, BMP-4 induced ALP activity at lower concentrations than in C2C12 myoblasts (Fig. 2E and F). As in C2C12 cells, ALP activity was much higher in the presence of the soluble fraction of PRP than that of PPP in both osteoblastic cell lines (Fig. 2E and F). 3T3-L1 preadipocytes also exhibited ALP activity on stimulation by the PRP fraction with more than 2 μg/ml of BMP-4 (data not shown).

Soluble PRP fraction stimulates osteoblastic differentiation of C2C12 cells cultured on scaffolds

BMPs are usually used in vivo with scaffolds made of collagen or hydroxyapatite to maintain local concentrations at sites of implantation [13,14]. We therefore pre-treated scaffolds of collagen sponge or hydroxyapatite with a mixture of BMP-4 and increasing amounts of the soluble PRP fraction. C2C12 cells were cultured on these scaffolds without additional BMPs or PRP. ALP activity was

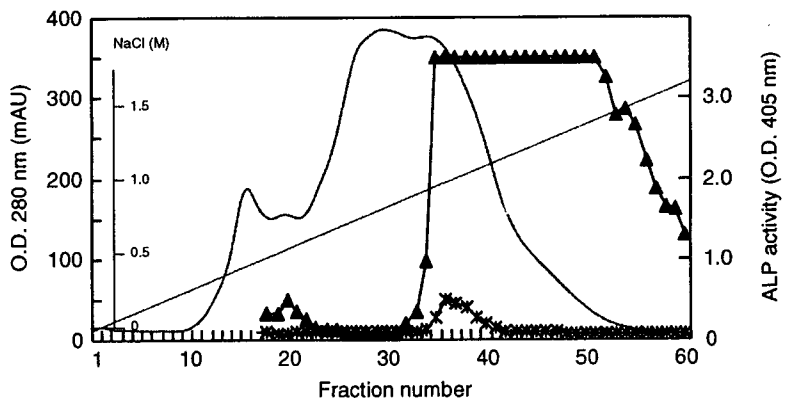

Fig. 4. BMP potentiator in CS binds to a heparin sepharose CL-6B column. Pre-fractionated CS was applied to a heparin sepharose CL-6B column as described in Materials and methods. The bound proteins were eluted by a linear gradient of NaCl from 0 to 2.0 M. Absorbance at 280 nm was monitored. The BMP potentiator activity in each fraction was determined by measuring ALP activity in C2C12 cells cultured with (triangles) or without (asterisks) 20 ng/ml of BMP-4.

induced on scaffolds pre-treated with the soluble PRP fraction and BMP-4, although enzyme activity gradually decreased with increasing amounts of the PRP fraction (Fig. 3A and B).

BMP potentiator in serum binds to a heparin sepharose CL-6B column

We have reported purification and identification of BMP-4 from bovine serum [11]. In our preliminary experiments, BMP potentiator was also detected in CS, which contains various factors released from platelets. To characterize the BMP potentiators, CS was applied to a heparin sepharose CL-6B column, and the bound proteins were eluted with a linear gradient of NaCl (Fig. 4). Fractions 35–53 induced high ALP activity in the presence of BMP-4 (Fig. 4). The potentiator activity on BMP-4 in a pool of the fractions 35–53 was lost by digestion with trypsin (data not shown).

Discussion

In the present study, we found that the soluble fraction prepared from activated PRP stimulates osteoblastic differentiation in the presence of BMPs in mesenchymal progenitor cells. Pretreatment of scaffolds with BMP-4 and the soluble PRP fraction stimulated osteoblastic differentiation in vitro. Because PRP is an autologous blood product, simultaneous application of PRP and BMPs with scaffolds may be a simple and useful method for enhancement of bone formation in vivo.

The stimulatory activity of PRP on bone healing in vivo is believed to be due to stimulation of proliferation of progenitor cells by growth factors released from activated platelets [8,9]. Interestingly, we found dual effects of the soluble fraction prepared from PRP on proliferation and differentiation. At lower concentrations, the PRP fraction markedly stimulated the osteoblastic differentiation in the presence of BMPs, while at higher concentrations the same fraction stimulated proliferation and suppressed osteoblastic differentiation. PDGF and TGF-β, which are abundantly stored in platelets, may be involved in stimulation of proliferation and suppression of differentiation, since such activities of PDGF and TGF-β have been reported in osteoblast progenitor cells [10,15,16]. These findings suggest that optimal dosages of PRP and BMPs must be determined to stimulate bone formation in vivo.

BMP activities are regulated positively and negatively by various types of molecules in the extracellular environment [17–19]. Although many inhibitors of BMPs have been identified as antagonists, such as noggin, chordin, follistatin, and the DAN family members, potentiators of BMPs have yet to be clearly identified [17–19]. We previously reported that some native and synthetic sulfated polysaccharides act as BMP potentiators in vitro and in vivo [6,7]. This activity is strongly dependent on both their size and the number of sulfated residues [6]. Recently, KCP, a Kielin/chordin-like protein, was identified as a novel BMP potentiator in the kidney [20]. KCP plays an important role in attenuating the pathology of renal fibrotic disease [21]. Our findings here suggest that platelets contain not only growth factors for proliferation but also novel potentiator(s) for BMP-dependent differentiation. Synergism between novel potentiator(s) in platelets and BMPs may also be involved in the stimulation of bone healing with use of PRP alone, since BMPs are present in bone matrix [22]. It is possible that a similar stimulation of the BMP activity by novel potentiator(s) plays an important role in native fracture healing in vivo. Identification of this novel potentiator and establishment of conditions of application of it with BMPs should enable clinically use of it for stimulation of local bone formation in vivo. Our findings suggested that this potentiator is a heparin-binding protein rather than a polysaccharide. This novel BMP potentiator produced by platelets is presently being studied in greater detail in our laboratory.

In conclusion, we found that PRP stimulates osteoblastic differentiation of mesenchymal progenitor cells in vitro in the presence of BMPs. Simultaneous administration of PRP and BMPs with scaffolds should be useful for stimulation of bone formation in vivo.

Acknowledgments

This work was supported in part by the Ministry of Education, Culture, Sports, Science and Technology of Japan, and in particular by a Ministry Grant to the Saitama Medical University Research Center for Genomic Medicine.

References

[1] T. Katagiri, T. Suda, K. Miyazono, The bone morphogenetic proteins, in: K. Miyazono, R. Derynck (Eds.), The TGF-β Superfamily Monograph, Cold Spring Harbor, New York, in press..
[2] J.T. Thomas, M.W. Kilpatrick, K. Lin, L. Erlacher, P. Lembessis, T. Costa, P. Tsipouras, F.P. Luyten, Disruption of human limb morphogenesis by a dominant negative mutation in CDMP1, Nat. Genet. 17 (1997) 58–64.
[3] T.D. Alden, P. Varady, D.F. Kallmes, J.A. Jane Jr., G.A. Helm, Bone morphogenetic protein gene therapy, Spine 27 (2002) S87–S93.
[4] P.S. Issack, P.E. DiCesare, Recent advances toward the clinical application of bone morphogenetic proteins in bone and cartilage repair, Am. J. Orthop. 32 (2003) 429–436.
[5] K. Kusumoto, K. Bessho, K. Fujimura, J. Akioka, Y. Okubo, Y. Wang, T. Iizuka, Y. Ogawa, Osteoinduction by recombinant human bone morphogenetic protein-2 in muscles of non-human primates, J. Int. Med. Res. 30 (2002) 251–259.
[6] T. Takada, T. Katagiri, M. Ifuku, N. Morimura, M. Kobayashi, K. Hasegawa, A. Ogamo, R. Kamijo, Sulfated polysaccharides enhance the biological activities of bone morphogenetic proteins, J. Biol. Chem. 278 (2003) 43229–43235.
[7] B. Zhao, T. Katagiri, H. Toyoda, T. Takada, T. Yanai, T. Fukuda, U.I. Chung, T. Koike, K. Takaoka, R. Kamijo, Heparin potentiates the in vivo ectopic bone formation induced by bone morphogenetic protein-2, J. Biol. Chem. 281 (2006) 23246–23253.
[8] L. Boyapati, H.L. Wang, The role of platelet-rich plasma in sinus augmentation: a critical review, Implant Dent. 15 (2006) 160–170.

[9] T.F. Tozum, B. Demiralp, Platelet-rich plasma: a promising innovation in dentistry, J. Can. Dent. Assoc. 69 (2003) 664.
[10] T. Katagiri, A. Yamaguchi, M. Komaki, E. Abe, N. Takahashi, T. Ikeda, V. Rosen, J.M. Wozney, A. Fujisawa-Sehara, T. Suda, Bone morphogenetic protein-2 converts the differentiation pathway of C2C12 myoblasts into the osteoblast lineage, J. Cell Biol. 127 (1994) 1755–1766.
[11] K. Kodaira, M. Imada, M. Goto, A. Tomoyasu, T. Fukuda, R. Kamijo, T. Suda, K. Higashio, T. Katagiri, Purification and identification of a BMP-like factor from bovine serum, Biochem. Biophys. Res. Commun. 345 (2006) 1224–1231.
[12] H. Hattori, M. Ishihara, T. Fukuda, T. Suda, T. Katagiri, Establishment of a novel method for enriching osteoblast progenitors from adipose tissues using a difference in cell adhesive properties, Biochem. Biophys. Res. Commun. 343 (2006) 1118–1123.
[13] Y. Kuboki, H. Takita, D. Kobayashi, E. Tsuruga, M. Inoue, M. Murata, N. Nagai, Y. Dohi, H. Ohgushi, BMP-induced osteogenesis on the surface of hydroxyapatite with geometrically feasible and nonfeasible structures: topology of osteogenesis, J. Biomed. Mater. Res. 39 (1998) 190–199.
[14] H. Toyoda, H. Terai, R. Sasaoka, K. Oda, K. Takaoka, Augmentation of bone morphogenetic protein-induced bone mass by local delivery of a prostaglandin E EP4 receptor agonist, Bone 37 (2005) 555–562.
[15] A.F. Kells, S.R. Coats, H.S. Schwartz, R.L. Hoover, TGF-beta and PDGF act synergistically in affecting the growth of human osteoblast-enriched cultures, Connect. Tissue Res. 31 (1995) 117–124.
[16] T. Katagiri, T. Lee, H. Takeshima, T. Suda, H. Tanaka, S. Omura, Transforming growth factor-beta modulates proliferation and differentiation of mouse clonal osteoblastic MC3T3-E1 cells depending on their maturation stages, Bone Miner. 11 (1990) 285–293.
[17] E. Abe, Function of BMPs and BMP antagonists in adult bone, Ann. N. Y. Acad. Sci. 1068 (2006) 41–53.
[18] V. Rosen, BMP and BMP inhibitors in bone, Ann. N. Y. Acad. Sci. 1068 (2006) 19–25.
[19] E. Gazzerro, E. Canalis, Bone morphogenetic proteins and their antagonists, Rev. Endocr. Metab. Disord. 7 (2006) 51–65.
[20] J. Lin, S.R. Patel, X. Cheng, E.A. Cho, I. Levitan, M. Ullenbruch, S.H. Phan, J.M. Park, G.R. Dressler, Kielin/chordin-like protein, a novel enhancer of BMP signaling, attenuates renal fibrotic disease, Nat. Med. 11 (2005) 387–393.
[21] M. Yanagita, Modulator of bone morphogenetic protein activity in the progression of kidney diseases, Kidney Int. 70 (2006) 989–993.
[22] M.R. Urist, Bone: formation by autoinduction, Science 150 (1965) 893–899.

Interleukin-4 inhibition of osteoclast differentiation is stronger than that of interleukin-13 and they are equivalent for induction of osteoprotegerin production from osteoblasts

Atsushi Yamada,[1] Masamichi Takami,[1] Tadaharu Kawawa,[2] Rika Yasuhara,[1] Baohong Zhao,[1] Ayako Mochizuki,[1,2] Yoichi Miyamoto,[1] Tomoo Eto,[3] Hisataka Yasuda,[4] Yuko Nakamichi,[5] Nacksung Kim,[6] Takenobu Katagiri,[7] Tatsuo Suda[7] and Ryutaro Kamijo[1]

Departments of [1]Biochemistry and [2]Prosthodontics, School of Dentistry, Showa University, Tokyo, Japan, [3]Reproductive Engineering Laboratory, Animal Resources and Development Department, Central Institute for Experimental Animals, Kawasaki, Japan, [4]Nagahama Institute for Biochemical Science, Oriental Yeast Co., Ltd, Nagahama, Japan, [5]Institute for Oral Science, Matsumoto Dental University, Shiojiri, Japan, [6]Medical Research Center for Gene Regulation, Chonnam National University Medical School, Gwangju, Korea and [7]Division of Pathophysiology, Research Center for Genomic Medicine, Saitama Medical School, Hidaka, Japan

Summary

Interleukin (IL)-4 and IL-13 are closely related cytokines known to inhibit osteoclast formation by targeting osteoblasts to produce an inhibitor, osteoprotegerin (OPG), as well as by directly targeting osteoclast precursors. However, whether their inhibitory actions are the same remains unclear. The inhibitory effect of IL-4 was stronger than that of IL-13 in an osteoclast-differentiation culture system containing mouse osteoblasts and osteoclast precursors. Both cytokines induced OPG production by osteoblasts in similar time- and dose-dependent manners. However, IL-4 was stronger in direct inhibition that targeted osteoclast precursors. Furthermore, IL-4 induced phosphorylation of signal transducer and activator of transcription-6 (STAT6) at lower concentrations than those of IL-13 in osteoclast precursors. IL-4 but not IL-13 strongly inhibited the expression of nuclear factor of activated T-cells, cytoplasmic 1 (nuclear factor-ATc1), a key factor of osteoclast differentiation, by those precursors. Thus, the activities of IL-4 and IL-13 toward osteoclast precursors were shown to be different in regards to inhibition of osteoclast differentiation, whereas those toward osteoblasts for inducing OPG expression were equivalent.

Keywords: IL-4; IL-13; osteoclasts; osteoblasts; cellular differentiation

doi:10.1111/j.1365-2567.2006.02538.x
Received 10 June 2006; revised 10 November 2006; accepted 13 November 2006.
Correspondence: Dr M. Takami, Department of Biochemistry, School of Dentistry, Showa University, 1-5-8 Hatanodai, Shinagawa, Tokyo 142–8555, Japan.
Email: takami@dent.showa-u.ac.jp
Senior author: R. Kamijo,
email: kamijor@dent.showa-u.ac.jp

Introduction

Osteoclasts are multinucleated giant cells that play a role in bone resorption during bone metabolism. Osteoclast differentiation is induced by the receptor activator of nuclear factor (NF)-κB ligand (RANKL), which is produced by osteoblasts/stromal cells.[1] Osteoblasts/stromal cells also produce osteoprotegerin (OPG), a decoy receptor for RANKL, which inhibits osteoclast differentiation by interrupting the interaction between RANKL and its receptor RANK.[2–4] OPG gene-deficient mice exhibit severe osteoporosis, because of the increase in number of osteoclasts.[5,6] Therefore, a balanced gene expression level of RANKL and OPG is critical for regulation of bone mineral density.

Many investigators have explored the mechanisms of osteoclast differentiation using coculture and bone marrow-derived macrophage (BMM) culture systems. In

Abbreviations: IL, interleukin; OPG, osteoprotegerin; BMC, bone marrow cell; BMM, bone marrow-derived macrophage; RANKL, receptor activator of nuclear factor κB ligand; NFATc1, nuclear factor of activated T-cells, cytoplasmic 1.

previous coculture systems, bone marrow cells (BMCs) and osteoblasts were cocultured in the presence of 1α,25-dihydroxyvitamin D_3 [1α,25-$(OH)_2D_3$], which induced the production of RANKL and suppressed that of OPG in osteoblasts.[7,8] Further, in a BMM culture system, BMMs that were shown to be identical to osteoclast precursors were cultured in the presence of M-CSF and RANKL proteins.[9] Although both culture systems produced osteoclasts, the coculture system is considered to be more effective for examining the role of osteoblasts in osteoclast differentiation, while the BMM culture system is useful to examine the direct actions of various factors toward osteoclast precursors.

It has been reported that lymphocyte-derived cytokines play critical roles during bone metabolism under physiological and pathological conditions.[10] IL-4 and IL-13, T helper 2 (Th2) cytokines, are pleiotropic lymphokines produced by antigen activated T cells that play particularly important roles in inflammatory and immune responses.[11] Because IL-4 and IL-13 share a common receptor complex, quite similar intracellular signals are activated by these cytokines.[10,12] In addition, binding of IL-4 to the receptor IL-4Rα induces heterodimerization with a common γ-chain (γc) (type I receptor complex) or IL-13Rα1 (type II receptor complex). On the other hand, binding of IL-13 to its receptor IL-13Rα1 with moderate affinity induces heterodimerization with IL-4Rα. Such dimerization of the receptors activates downstream signalling molecules, including Janus kinase-1 (JAK1) and -3, and signal transducer and activator of transcription-6 (STAT6).[12] However, the expression levels of the receptors for IL-4 and IL-13 are regulated differently depending on cell type.

IL-4 is known to suppress RANKL-induced osteoclast differentiation through direct action on osteoclast precursors.[13] Recently, Palmqvist *et al.* reported that both IL-4 and IL-13 inhibited osteoclast differentiation by a mechanism that increased OPG in osteoblasts, and also decreased RANKL and RANK expression.[14]

In the present study, we compared the effects of IL-4 and IL-13 toward the inhibition of osteoclast differentiation using both coculture and BMM culture systems. Our results suggest that IL-4 is more effective than IL-13 toward osteoclast precursors, while they are equivalent in regards to stimulation of OPG production from osteoblasts.

Materials and methods

Chemicals

Recombinant murine IL-4 and IL-13, and transforming growth factor-β (TGF-β) were purchased from R & D systems (Minneapolis, MN). Alpha-modified minimum essential medium (α-MEM) and 1α,25$(OH)_2D_3$ were purchased from Sigma (St. Louis, MO). Human macrophage colony-stimulating factor (M-CSF, Leukoprol®) was purchased from Kyowa Hakko Kogyo (Osaka, Japan). The soluble form of human TRANCE (human RANKL) was a kind gift from Dr Yongwon Choi (University of Pennsylvania School of Medicine).[15,16]

Cell cultures

Primary calvarial osteoblasts were obtained from the calvariae of neonatal ddY mice (Saitama Experimental Animals, Saitama, Japan) using 0·1% collagenase and 0·2% dispase.[17] BMCs were obtained from the long bones of 4- to 6-week-old ddY male mice. To obtain BMMs, BMCs were cultured for 3 days in α-MEM containing 10% fetal bovine serum (Sigma), M-CSF (50 ng/ml), and TGF-β (1 ng/ml) in 100-mm diameter type-I collagen-coated culture dishes (IWAKI-Asahi Glass, Tokyo, Japan) (1×10^7 cells/dish). After culturing for 3 days, cells attached to the culture plates were collected and used as BMMs. In the BMM culture system, BMMs were cultured on 96-well cell culture plates (Corning, Corning, NY) in the presence of M-CSF (50 ng/ml) and RANKL (150 ng/ml) for 4 days. In the coculture system, BMMs (2×10^4 cells/well) or BMCs (1×10^5 cells/well) were cultured on 96-well cell culture plates (Corning) with mouse primary osteoblasts or cells from the stromal/osteoblastic cell line UAMS-32 (5×10^3 cells/well), in the presence or absence of 1α,25-$(OH)_2D_3$ (10 nM) for 6 days. After culturing, some of the cells were fixed and stained for tartrate-resistant acid phosphatase (TRAP), a marker enzyme of osteoclasts.

Measurement of TRAP activity

Cells in a 96-well culture plate were rinsed with phosphate-buffered saline and dissolved with 150 μl of lysis buffer (50 mM acetic acid buffer, pH 5·0, containing 1% sodium tartrate and 0·1% Triton-X). The cell lysates were briefly sonicated, then 20 μl of cell lysate was mixed with 100 μl of *p*-nitrophenyl phosphate solution (1 mg/ml in 50 mM acetic acid buffer, pH 5·0, containing 1% sodium tartrate) and incubated at 37° for 30 min. After the addition of 50 μl of 1 M NaOH, absorbance was measured at 405 nm.

Reverse transcriptase–polymerase chain reaction (RT–PCR)

Total RNA (1 μg) was reverse-transcribed using Superscript II (Invitrogen Life Technologies, Carlsbad, CA) according to the manufacturer's protocols. PCR was performed using Taq DNA polymerase (Sigma) under the following conditions: denaturation at 94° for 30 s, annealing at 58° for 30 s, and extension at 72° for 30 s, with

25 cycles for glyceraldehyde 3-phosphate dehydrogenase (GAPDH) and 30 cycles for mouse IL-4Rα, γ_c, IL-13Rα1, and NFATc1. The oligonucleotide primers used for RT–PCR were as follows:

GAPDH (452 bp), 5′-GAAGGTCGGTGTGAACGGATTTGGC-3′ and 5′-CATGTAGGCCATGAGGTCCACCAC-3′; mouse IL-4Rα (432 bp), 5′-ATCTGCGTGCTTGCTGGTTCT-3′ and 5′-CTGGTATCTGTCTGATTGGACCG-3′; mouse γc (266 bp), 5′-GTTCTGAGCCTCAGGCAACC-3′ and 5′-CAGATTGCTGAGTGTTAGAT-3′; mouse IL-13Rα1 (385 bp), 5′-CATCTTCTCCTCAAAAATGGTGCC-3′ and 5′-GGATTATGACTGCCACTGCGAC-3′; and mouse NFATc1 (565 bp), 5′-TCATCCTGTCCAACACCAAA-3′ and 5′-TTGCGGAAAGGTGGTATCTC-3′.

Northern blot analysis

Ten micrograms of total RNA was extracted from the cells and electrophoresed on a 1% agarose gel containing 0·22 M formaldehyde, then blotted onto nylon membranes (Hybond-N, Amersham Biosciences, Amersham, UK). Filters were serially hybridized with cDNA probes for mouse OPG, RANKL, and 18S rRNA, then hybridization was performed in Perfect Hybridization Solution (Sigma) overnight at 65°. The membranes were washed twice with 2× saline sodium citrate (SSC) containing 0·1% sodium dodecyl sulphate (SDS) at 65° for 30 min and once with 2× SSC at 65° for 30 min, followed by exposure to a storm phosphoimager screen (Molecular Dynamics, Sunnyvale, CA). Signals were visualized and quantitated using ImageQuant software (Molecular Dynamics).

Western blot analysis

Western blot analysis was performed as described previously.[18] Briefly, the lysates of BMMs and UAMS-32 cells treated with various concentrations of IL-4 and IL-13 were subjected to 10% SDS–polyacrylamide gel electrophoresis and transferred to Immobilon-P membranes (Millipore, Billerica, MA). The membranes were incubated with antibodies against murine STAT6 and phospho-STAT6 (Cell Signaling Technology, Beverly, MA), following incubation with horseradish peroxidase-conjugated secondary antibody (Cell Signaling Technologies). Protein bands were detected by use of ECL plus Western Blotting Detection system (Amersham Biosciences) and exposed to a FUJI medical X-ray film (FUJIFILM, Kanagawa, Japan).

Quantification of OPG

Cells were cultured for various periods with increasing amounts of OPG. The amount of OPG released into the culture medium was determined using a mouse OPG/TNFRSF11B Immunoassay kit (R & D Systems, Inc.) according to the manufacturer's instructions.

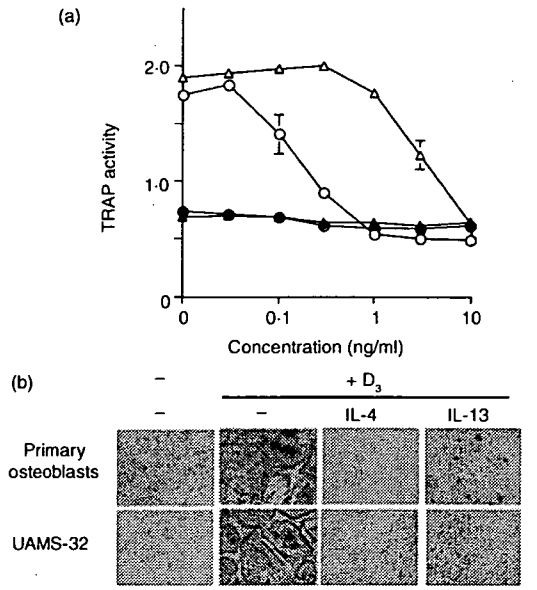

Figure 1. Effects of IL-4 and IL-13 on osteoclast differentiation in a coculture system. (a) BMMs were cocultured with UAMS-32 cells and various concentrations of IL-4 (○) or IL-13 (△) in the presence of 100 nM 1α,25-$(OH)_2D_3$. The same cultures were also performed in the absence of 1α,25-$(OH)_2D_3$ (D_3) with IL-4 (●) or IL-13 (▲). After culturing the cells, cell lysates were harvested and TRAP activity was measured. Data are shown as the means ± SE ($n = 4$). (b) BMMs cocultured with primary osteoblasts or UAMS-32 cells in the absence or presence of 10 nM of 1α,25-$(OH)_2D_3$ (D_3), 10 ng/ml of IL-4 or 10 ng/ml IL-13. The cells were fixed and stained for TRAP (original magnification: ×10).

Results

Inhibition of osteoclast differentiation by IL-4 and IL-13 in coculture system

We first examined the effects of IL-4 and IL-13 on osteoclast differentiation in a coculture system, in which mouse BMMs were cultured with UAMS-32 cells in the presence of 1α,25-$(OH)_2D_3$, an inducer of RANKL expression. The addition of IL-4 at a concentration of 1 ng/ml to the cocultures completely inhibited osteoclast differentiation, whereas 10 ng/ml of IL-13 was required for complete inhibition (Fig. 1a, b). The IC_{50} values of IL-4 and IL-13 for osteoclast differentiation were 0·13 and 2·69 ng/ml, respectively (Fig. 1a). These results suggest that the inhibitory activity of IL-4 is stronger than that of IL-13 in the coculture system.

Regulation of OPG and RANKL expression in osteoblasts by IL-4 and IL-13

Because OPG produced by osteoblasts is a potent inhibitor of osteoclast differentiation, we examined the expression levels of OPG mRNA before and after treatment